Dynamic modeling of the transition from passive to active rifting, application to the Pannonian Basin

Article *in* Tectonics · December 2001

DOI: 10.1029/2001TC900010

CITATIONS
146

READS
174

3 authors, including:

Ritske Huismans
University of Bergen
132 PUBLICATIONS **3,878** CITATIONS

SEE PROFILE

TECTONICS, VOL. 20, NO. 6, PAGES 1021-1039, DECEMBER 2001

Dynamic modeling of the transition from passive to active rifting, application to the Pannonian basin

Ritske S. Huismans[1]
Institute of Earth Sciences, Vrije Universiteit, Amsterdam, Netherlands

Yuri Y. Podladchikov
Geologisches Institut, ETH-Zentrum, Zurich, Switserland

Sierd Cloetingh
Institute of Earth Sciences, Vrije Universiteit, Amsterdam, Netherlands

Abstract. We examine a number of first-order features of Pannonian basin evolution in terms of the feedback relation between passive far-field-induced extension and active Raleigh Taylor instable upwelling of the asthenosphere. We show that active mantle upwelling following a phase of passive extension are viable mechanisms explaining the Pannonian basin formation. The dynamic interplay between far-field-driven passive extension and active thinning of the mantle lithosphere by convective upwelling beneath the rift zone is modeled using thermomechanical finite element methods. Our modeling results predict a first phase of passive lithospheric thinning which is followed by a second phase of late synrift to postrift active mantle lithosphere thinning due to buoyancy-induced flow beneath the rift zone. We argue that the pattern of coeval extension in the thinning region and compression in the flanking regions may be explained by the buoyancy forces due to lithosphere thinning. It is demonstrated that timescales of and stresses generated by both processes are comparable. The model appears also to explain the occurrence of late shallow mantle-related decompression melts in the Pannonian region and late regional doming.

1. Introduction

Thinning of the lithosphere, rifting, and continental breakup have long been considered in terms of two end-member groups of models, active rifting models and passive rifting models (Figure 1) [*Sengor and Burke,* 1978; *Turcotte,* 1983]. In the first group, convective upwelling of the asthenosphere drives rifting, a mantle plume impinging on the base of the lithosphere drives continental breakup. In these models, local buoyancy forces generate the tensional stresses able to break the lithosphere [*Houseman and England,* 1986]. In the second group of models, horizontal, in-plane far-field forces, possibly due to large-scale plate interactions, initialize and drive lithosphere extension and rifting [*Cloetingh and Wortel,* 1986].

The relative timing of rifting and rift-related volcanism was used to discriminate between these two basic types of rifting [*Sengor and Burke,* 1978]. In rift zones where doming and volcanism precede rifting, an active mantle plume was believed to act on the base of the lithosphere. In contrast, in rift zones where volcanism and doming succeed rifting, the asthenosphere was assumed to play a passive role, filling the space created by localized extension. *Sengor and Burke* [1978] stated that the passive mode of rifting is by far the more widespread of the two.

Application of the original McKenzie model [*McKenzie,* 1978] to extensional basins showed substantial deviations from the model predictions [*Royden and Keen,* 1980; *Sclater et al.,* 1980; *Beaumont et al.,* 1982; *Kooi,* 1991]. In order to explain minor or absent synrift subsidence and/or very high subsidence in the postrift in, for instance, the North Sea, the Labrador Sea, the Pannonian basin, and many other basins the differential stretching model was proposed [*Royden and Keen,* 1980; *Beaumont et al.,* 1982] in which the crust and the mantle lithosphere are allowed to thin by different amounts. In general, additional subcrustal heating, i.e., mantle lithosphere thinning in the late synrift/postrift is needed to predict the observed basin stratigraphy. This is especially true for the Pannonian basin, which forms the focus of the present paper.

The Neogene Pannonian basin (Figure 1) has since long been recognized as a key area for studying the evolution of rift basins. Its intermediate extension and the

[1]Now at Department of Oceanography, Dalhousie University, Halifax, Nova Scotia, Canada.

Paper number 2001TC900010.
0278-7407/01/2001TC900010$12.00

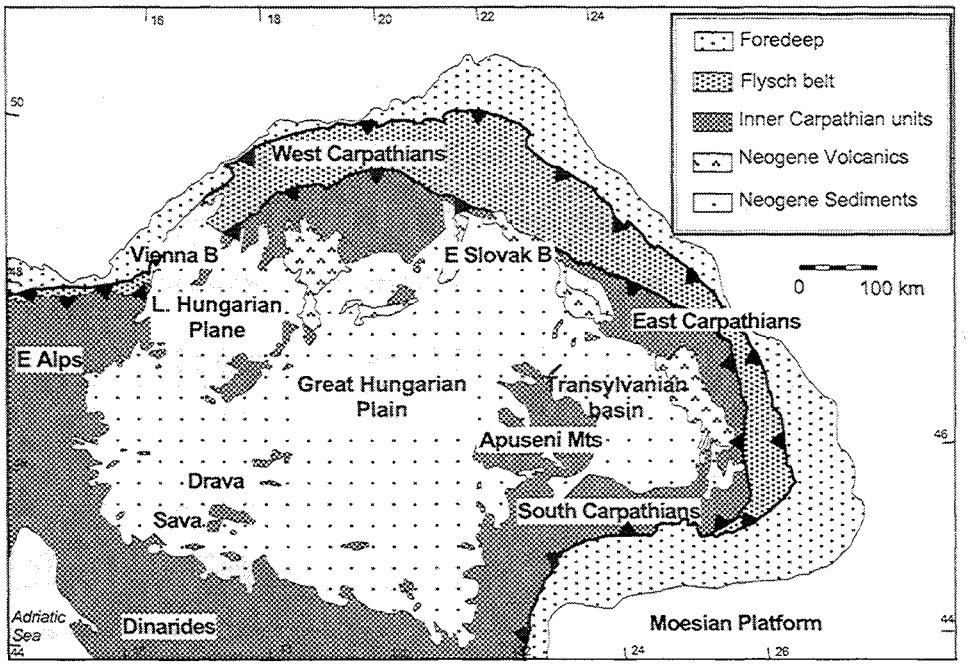

Figure 1. Overview of regional geology and geography of the Pannonian basin system after *van Balen and Cloetingh* [1995].

coeval occurrence of compression and subduction in the surrounding Carpathian and Dinaric chains characterize it as an intramontane rift basin. The availability of an extensive high-quality database on crustal and lithospheric thickness, synrift and postrift fill, heat flow, stratigraphic control and its sedimentary, and structural evolution make it particularly well suited for study of the dynamics of basin formation [*Royden et al.,* 1982; *Horvath,* 1993].

The main features characterizing the Pannonian basin pose a general problem in terms of extensional basin formation processes, e.g., the coeval occurrence of extension and compression, the strong differential thinning of the lithosphere beneath the Pannonian basin, its active postrift evolution and the succession of calc-alkaline volcanics in the synrift stage by alkaline volcanics in the late synrift to postrift stage. In terms of existing dynamic models the Pannonian basin is still enigmatic, and until now, no quantitative dynamic modeling attempt has been undertaken predicting the first-order features characteristic of the region.

Passive rifting in a back arc extensional setting, which has been proposed to explain the main features of the Pannonian basin [*Royden et al.,* 1983b], may successfully explain only part of the observables, e.g., the crustal thinning pattern and the extensional features at the surface. The strong differential stretching, the late mantle-related volcanic activity, and the coeval postrift second phase of extension and postrift climax in compression in the east Carpathians, however, cannot be explained by a simple passive rifting model alone [*van Bemmelen,* 1973; *Stegena et al.,* 1975; *Huismans,* 1999].

In order to explain these latter features, several authors envisaged a mantle plume operating beneath the Pannonian basin [*van Bemmelen,* 1973; *Stegena et al.,* 1975]. However, since the mantle-related features of the Pannonian basin system develop subsequent to the initiation of the passive rift, it appears that asthenospheric doming is a consequence of the previous rifting history and the role of a deep mantle plume must be ruled out.

Asthenospheric doming following the initiation of the rift zone is supported from a physical point of view since the lithosphere-asthenosphere boundary is basically unstable and, following a phase of lithospheric thinning, has the tendency to move upward in a diapiric mode [*Keen,* 1985; *Buck,* 1985]. This is due to the density inversion over the lithosphere-asthenosphere boundary; that is, the shallow asthenosphere has a lower density then the mantle lithosphere. In the following, it will be shown that a number of first-order features of the Pannonian basin can be explained by a first phase of passive extension followed by a second phase of active small-scale convective upwelling of the asthenosphere beneath the rift zone induced by the previous rifting history [*Buck,* 1985, 1986; *Keen and Boutilier,* 1995].

We first discuss in more detail the tectonic setting and the temporal evolution of the Alpine-Carpathian-Pannonian system. Subsequently, the numerical results are presented and compared with the general features of the region.

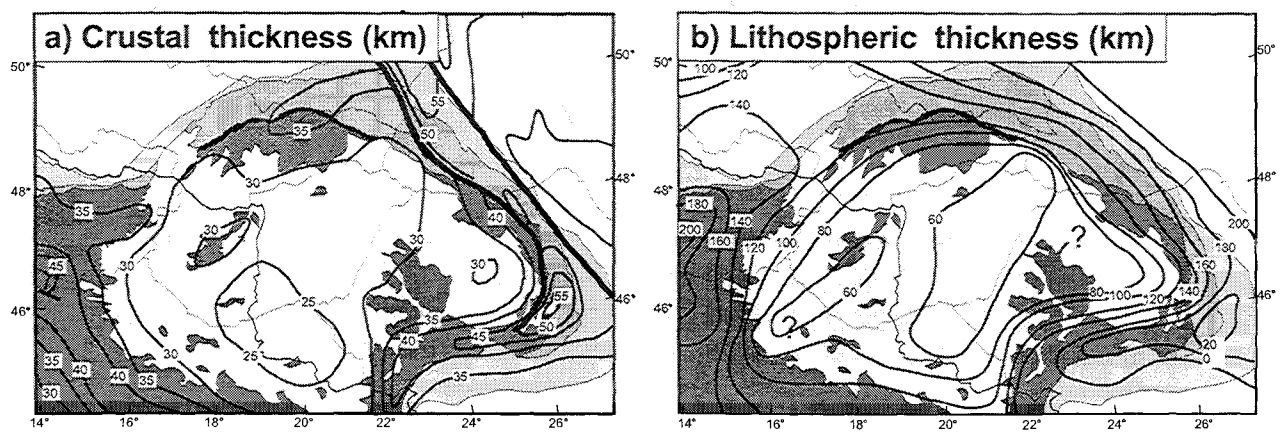

Figure 2. (a) Crust and (b) mantle lithosphere thickness in the Pannonian region [after *Horvath,* 1993]. Note the very high gradients in lithosphere thickness in the eastern and western part of the system.

2. Pannonian Basin, Tectonic Setting, Regional Geologic Evolution, and Geological Data

Following a complex history of thickening and local basin formation from the late early Cretaceous until the early Miocene (100-19.5 Ma), extension in the Pannonian basin initiated on previously thickened crust and lithosphere [*Stegena et al.,* 1975; *Sclater et al.,* 1980; *Royden et al.,* 1982; *Horvath,* 1993]. Strongest mantle lithosphere and crustal thinning have occurred in two NNE-SSW trending zones in the center of the basin (Figures 2a and 2b). At present, the Pannonian basin is characterized by anomalous high heat flow values [*Sclater et al.,* 1980; *Lenkey,* 1999].

The Neogene tectonic history of the Pannonian Carpathian system can be summarized in the following four main phases [*Royden,* 1983a, 1983b; *Csontos,* 1995]: (1) prerift thickening in the late Oligocene to early Miocene, with N-S to NW-SE compression, (2) middle to late Miocene first extensional phase, (3) late Miocene to Pliocene short phase of inversion followed by the second phase of extension coeval with climax of compression east and south Carpathians, and (4) Pliocene to Quaternary inversion and locking of the Pannonian basin system. We include a stratigraphic time table (Figure 3), correlating the Neogene timescale with the Eastern Parathetys one.

2.1. Structural Evolution

The last major tectonic event before the onset of extension in the Pannonian basin is a widespread phase of N-S to NW-SE compression (Figure 4a). At this stage the different microplates comprising the internal parts of the Pannonian area were assembled, producing an initial thickening of the prerift lithosphere. In the eastern part of the system an embayment of thinned continental crust or oceanic crust was preserved north of the Moesian platform. Renewed initiation of westward subduction in the east Carpathian arc accommodated eastward movement of the Pannonian prerift lithosphere, leading to the first phase of extension.

The first phase of extension in the Pannonian basin took place in the middle to late Miocene between 17.5 and 14 Ma (Figures 4b and 4c) [*Horvath,* 1995]. Pull-apart basins developed along major NE and SW oriented fault zones in an extensional strike-slip regime along the borders of the Pannonian basin in the Karpathian (17.5-16.5 Ma) (Figure 4b). Subsequently, in the Badenian (16.5-14 Ma) the central Pannonian basin area was affected by pure E-W extension (Figure 4c). Local very deep basins developed, associated with crustal thinning [*van Balen and Cloetingh,* 1995]. On a regional scale the crust and lithosphere were thinned in a more gradual way.

A mid-Badenian (14 Ma) unconformity has been interpreted to mark the end of rifting [*Horvath,* 1995]. At the same time, eastward escape and strike slip occurred in the Eastern Alps and the west Carpathians [*Royden et al.,* 1982; *Ratschbacher et al.,* 1991a; *Lankreijer et al.,* 1995].

Although basins where locally affected by either NE-SW or NW-SE directed extension, on a larger scale the local subbasins accommodated an overall E-W extension that affected the whole region between the Eastern Alps and the east Carpathians [*Bergerat,* 1989; *Huismans et al.,* 1997; *Peresson and Decker,* 1997a].

In the early/middle Sarmatian the Pannonian basin was affected by a compressional event (Figure 4d) [*Horvath,* 1995]. Uplift and intensive erosion is documented by the absence of Sarmatian sediments in many parts of the Pannonian basin. Subsidence and sedimentation

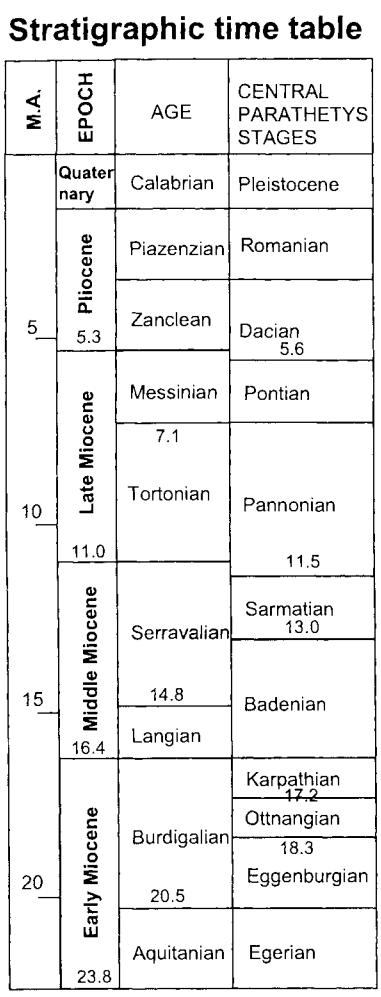

Figure 3. Time table with correlation of central Parathetys stages with standard age definitions [after *Rögl*, 1996].

were again reestablished in the early Pannonian. The stress field during inversion is characterized by ENE-WSW to E-W compression [*Fodor et al.*, 2000]. This was coeval with the start of major compression in the east Carpathians in the early/middle Sarmatian (13.5-11.5 Ma).

E-W extensional structures found in the central and western parts of the Pannonian basin (Figure 4e) [*Fodor et al.*, 2000] and accelerated subsidence and sedimentation rate of the main subbasins of the area [*Lankreijer et al.*, 1995] document a second phase of extension for the late Miocene to early Pliocene (11.5-8(?) Ma). Coeval with this second extensional phase, a strong compressional pulse affected the region to the east and to the west of the Pannonian basin [*Huismans et al.*, 1996; *Peresson and Decker*, 1997a; *Sanders et al.*, 1999].

Finally, the Pannonian basin became locked during the late Pliocene to Recent (Figure 4f), and the region experienced a compressional stress field with varying stress orientations [*Muller et al.*, 1992]. In the central and western Pannonian basin, however, transtension to E-W extension has been documented in basalts as young as 2 Ma [*Fodor et al.*, 2000].

2.2. Constraints From Basin Analysis

Several studies document the Neogene subsidence and sedimentation history of the main subbasins of the Pannonian basin system [*Sclater et al.*, 1980; *Royden et al.*, 1983b; *Lankreijer et al.*, 1995; *Sachsenhofer et al.*, 1997]. Typical subsidence histories for the border and central basin areas are illustrated in Figures 5a-d [*Royden et al.*, 1983b; *Lankreijer et al.*, 1995].

Whereas the first Karpathian to Badenian (17.5-14 Ma) rift phase affected the basins located at the borders of the Pannonian basin as well as the central Pannonian basin, the second early Pannonian (11.5-8(?) Ma) rift phase is only evident in the central parts of the Pannonian basin. During the first rift phase, crust and lithosphere were thinned by equal amounts with β and δ factors of the order 1.4-1.6 [*Royden et al.*, 1983b; *Lankreijer et al.*, 1995](e.g., Figures 5a and 5b).

After a period of no deposition and/or erosion, coeval with the phase of inversion in the late Sarmatian-early Pannonian, the second rift phase affected predominantly the central parts of the Pannonian basin in the early Pannonian (Figures 5c and 5d) [*Royden et al.*, 1983b; *Lankreijer et al.*, 1995]. For this phase, strong differential thinning of the mantle lithosphere of the order of $\delta = 4$-8 is required to explain the observations [*Sclater et al.*, 1980; *Royden et al.*, 1983b; *Lankreijer et al.*, 1995], whereas only minor additional thinning affected the crust. The strong spatial correlation between areas affected by the second rift phase and extreme lithospheric thinning clearly indicates a causal relation between asthenospheric updoming and the second rift phase.

2.3. Volcanism

The Neogene development of the Pannonian basin was accompanied by strong volcanic activity [*Szabo et al.*, 1992; *Balogh et al.*, 1994; *Downes and Vaselli*, 1995; *Embey-Isztin and Dobosi*, 1995; *Pecskay et al.*, 1995; *Vaselli et al.*, 1995]. Three volcanic suites can be distinguished: (1) early Miocene mainly acidic calc alkaline ignimbrites and tuff deposits, which extend over most of the Pannonian basin, the Transylvanian basin, and their margins, (2) middle Miocene to Recent calc-alkaline volcanics, which occur in the inner west Carpathians and in a linear belt parallel to the east Carpathian thrust belt (Figure 6a), and (3) late Miocene to Recent alkaline basalts, which occur in a more diffuse pattern over the Pannonian region (Figure 6b).

Neogene Stress and Strain Patterns in the Pannonian basin

Prerift collision, thickening and fore- and hinter-land basin formation

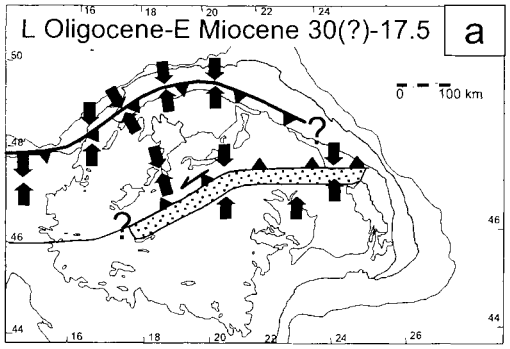

Early synrift, extensional strike slip

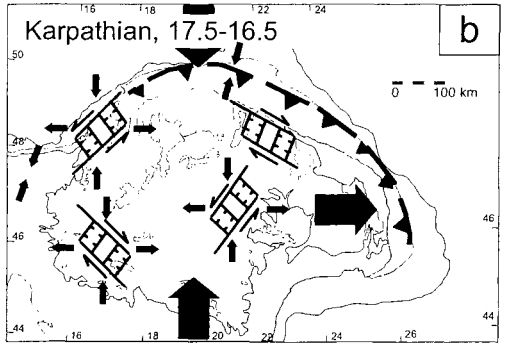

1st riftphase, pure extension

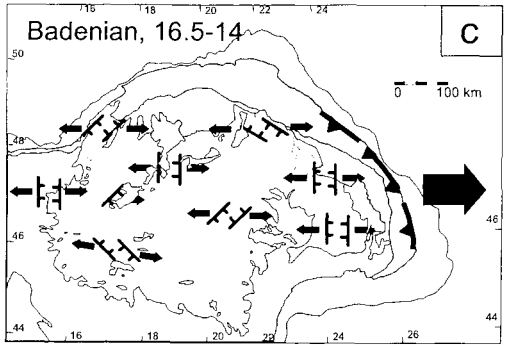

Inversion & start climax compression

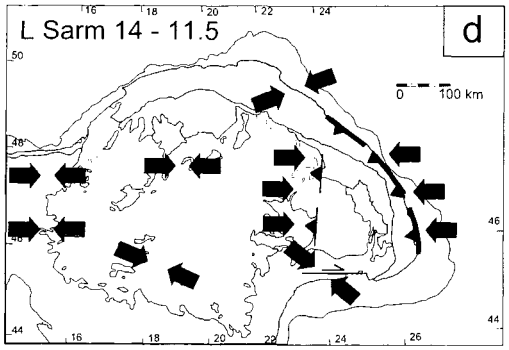

2nd rifting phase/climax compression

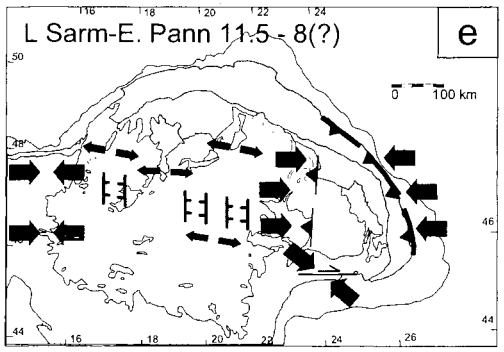

Quaternary inversion

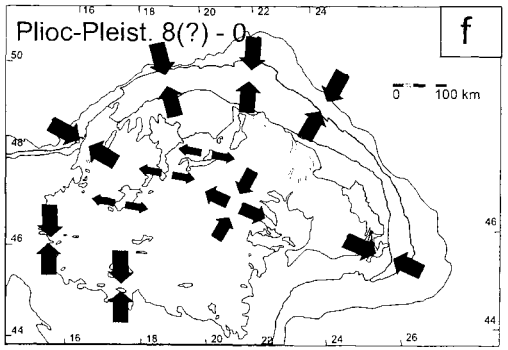

Figure 4. Structural evolution of the Pannonian basin area. Data compilation is after *Bergerat* [1989], *Csontos et al.* [1991], *Ratschbacher et al.* [1993], *Csontos* [1995], *Hippolyte and Sandulescu* [1996], *Huismans et al.* [1997], *Matenco* [1997], *Peresson and Decker* [1997a, 1997b], *Huismans* [1999], and *Fodor et al.* [2000]. (a) Late Oligocene-early Miocene prerift thickening, (b) early Miocene first extension phase, transtensional initiation of basin formation, (c) middle Miocene, continuation of first extension phase, pure E-W extension, (d) late Miocene, moderate inversion and start climax of compression in the east Carpathians, (e) late Miocene, second phase of extension and coeval compression, and (f) Pliocene-Quaternary basin inversion.

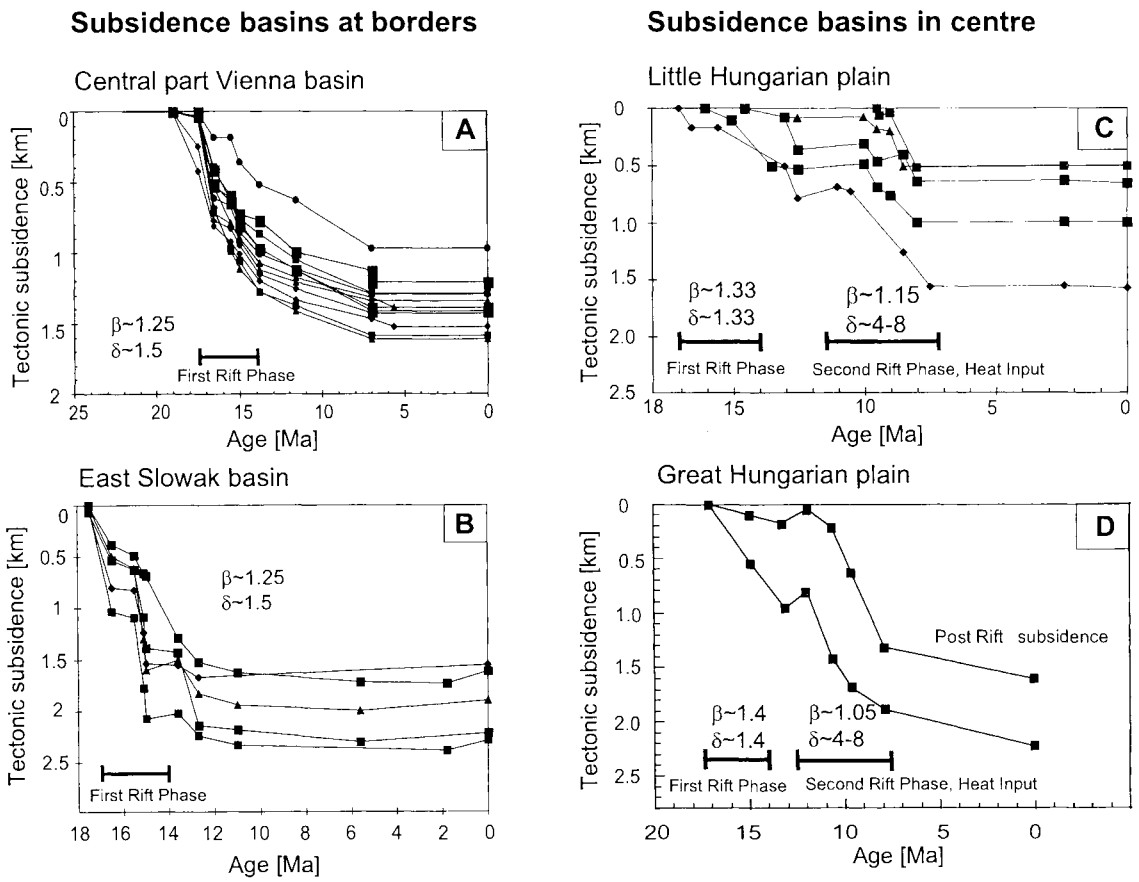

Figure 5. Contrasting tectonic subsidence and crustal and mantle lithosphere thinning factors β and δ at the borders of the Pannonian basin and in the central basin areas. Data are after *Lankreijer et al.* [1995] (Figures 5a-c) and *Royden et al.* [1982] (Figure 5d). (a) The Vienna basin, (b) the east Slowak basin, (c) the little Hungarian plain, and (d) the Great Hungarian plain. Note during first rift phase (17.5-14 Ma) homogeneous thinning. During second rift phase (12-8 Ma) strong differential thinning in the central Pannonian basin (Figures 5c and 5d) contrasts with homogenous thinning at the borders (Figures 5a and 5b).

The occurrence of calc-alkaline volcanism is diachronous with younger ages going from the west Carpathians toward the southeast Carpathians (Figure 6a). In the west Carpathians, ages range from middle Karpathian to the late Sarmatian/early Pannonian (17.5-9.6 Ma), whereas in the internal parts of the east Carpathians, ages range from middle Badenian to Recent (15-0.5 Ma). This volcanic suite is generally interpreted to be related to underthrusting and subduction of the east European foreland crust beneath the Pannonian basin.

The first occurrence of alkaline basaltic magmatism is around 11.5 Ma, coeval with the second rift phase and with strong mantle lithosphere upwelling (Figure 6b). Most important occurrences are in the Balaton highlands and in the Graz basin, slightly west of the center of maximum thinning in the Pannonian basin [*Downes and Vaselli,* 1995]. Ages range from 11.5 to 0.5 Ma, with a peak in the Pannonian around 7-8 Ma [*Szabo et al.*, 1992; *Balogh et al.*, 1994; *Pecskay et al.*, 1995].

Geochemical analysis of the alkaline volcanics points to a shallow asthenospheric source [*Downes and Vaselli,* 1995; *Embey-Isztin and Dobosi,* 1995; *Dobosi et al.*, 1995]. The small volumes of the basaltic lavas and low eruption rates indicate that the potential temperature of the asthenosphere was probably not higher then normal.

3. Previous Models and Outstanding Questions for the Formation of the Pannonian Basin System

We focus on two closely interrelated questions pertaining to the Pannonian basin system evolution. (1) What is the responsible process for strong mantle lithosphere thinning during the second rift phase? (2) What

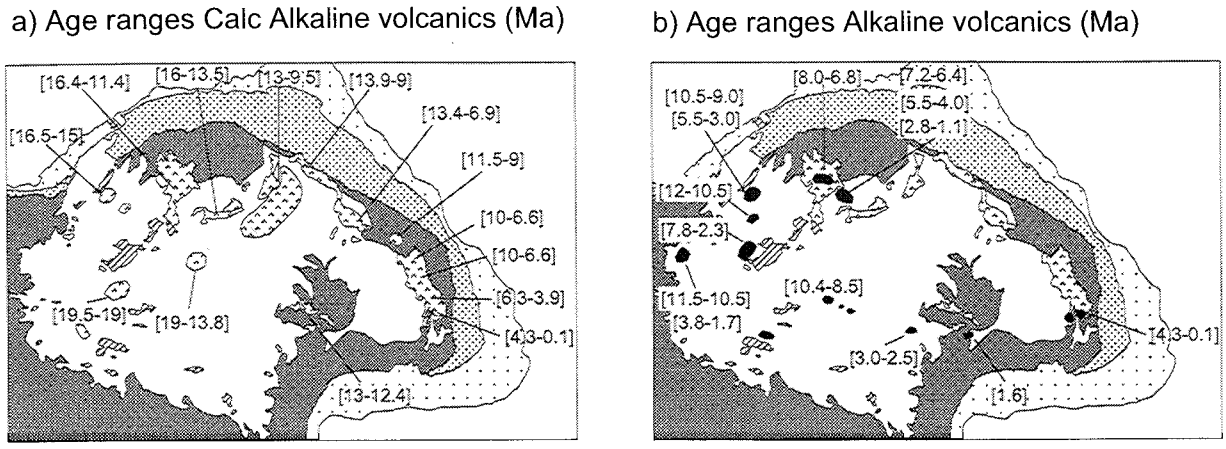

Figure 6. Age ranges of volcanic activity in the Pannonian basin system. Data are compiled from *Szabo et al.* [1992], *Balogh et al.* [1994], *Downes and Vaselli* [1995], and *Pecskay et al.* [1995]. (a) Calc-alkaline volcanics (Ma). Note younging along the Carphathian arc toward the east. (b) Alkaline volcanics (Ma) indicated by black dots. Note younger ages then the calc-alkaline volcanics and two peaks in alkaline volcanic activity (10 and 2-0 Ma).

is the driving force for the coeval second phase of rifting in the Pannonian basin and the climax of compression in the east Carpathians?

Earlier models proposed to explain part or all of the Pannonian basin system evolution fall into three distinct classes: (1) Eastern Alps collapse and escape models, where the Eastern Alpine crust is thought to have moved for > 200 km in the open oceanic (?) embayment of the Pannonian region [*Ratschbacher et al.,* 1991a, 1991b], (2) back arc extension models relating the extensional history of the Pannonian basin to subduction and a retreating slab beneath the east Carpathian arc [*Sclater et al.,* 1980; *Royden et al.,* 1983b; *Horvath,* 1993], and (3) models related to active mantle upwelling beneath the Pannonian basin [*van Bemmelen,* 1973; *Stegena et al.,* 1975; *Huismans,* 1999]. In the following, we will first give estimates of the amount of Eastern Alps extrusion to the east. Subsequently, we present dynamic modeling of the two-stage extensional history of the Pannonian basin. Finally, the results will be summarized, and the merits of back arc extension models and asthenosphere diapir models for the tectonics of the Pannonian basin system will be discussed in view of the presented results.

A simple area balancing of convergence in the east Carpathian arc with extension in the Pannonian basin area may give an estimate of the amount of space available for extrusion of the Eastern Alps to the east. Restoring the east Carpathian thrust belt to the early Miocene prerift configurations gives an estimate of 150-200 km eastward translation of the thrust belt (Figure 7a) [*Ellouz and Roca,* 1994].

We consider a section reaching from the east Carpathians in the east to the Eastern Alps in the west (Figure 7b). The assumption that extension and compression take place in a two-dimensional plane is justified by the fact that although, on a local scale, extension directions varied considerably, overall extension and contraction occurred in an E-W direction (e.g., see section 2.2 and *Bergerat* [1989]). Taking the crustal stretching factor β as the final length X_t of the region undergoing extension divided by the initial length X_0, an estimate of the initial length is given by

$$X_0 = \frac{X_t}{\beta}. \tag{1}$$

The mean value of crustal thinning is of the order of β = 1.6-1.8 [*Royden et al.,* 1983b; *Lankreijer et al.,* 1995]. The final length of the thinned region is in the range 350-550 km. With a final length of X_t = 350 km the initial length X_0 is in the range 190-220 km, whereas X_t = 550 km results in X_0 = 310-350 km. In this approximation the amount of possible eastward movement of the Eastern Alps, X_{escape}, is given by the amount of translation of the east Carpathians, D_x, minus the length change of the Pannonian region (Figure 7b):

$$X_{\text{escape}} = D_x - (X_t - X_0). \tag{2}$$

The amount of escape obtained in this way is in the range 0-50 km. This is much less then the proposed 200 km of Eastern Alpine escape to the east [*Ratschbacher et al.,* 1991a]. Although, obviously, three-dimensional effects may be important, overall extension and compression occurred in an E-W direction, and (2) gives a first-order estimate of the amount of eastward movement of the Eastern Alps. Large lateral eastward motion has been proposed for the north Pannonian unit. Among other arguments the estimates given above suggest that these translations occurred in the prerift history. For this reason, it appears that Eastern Alpine

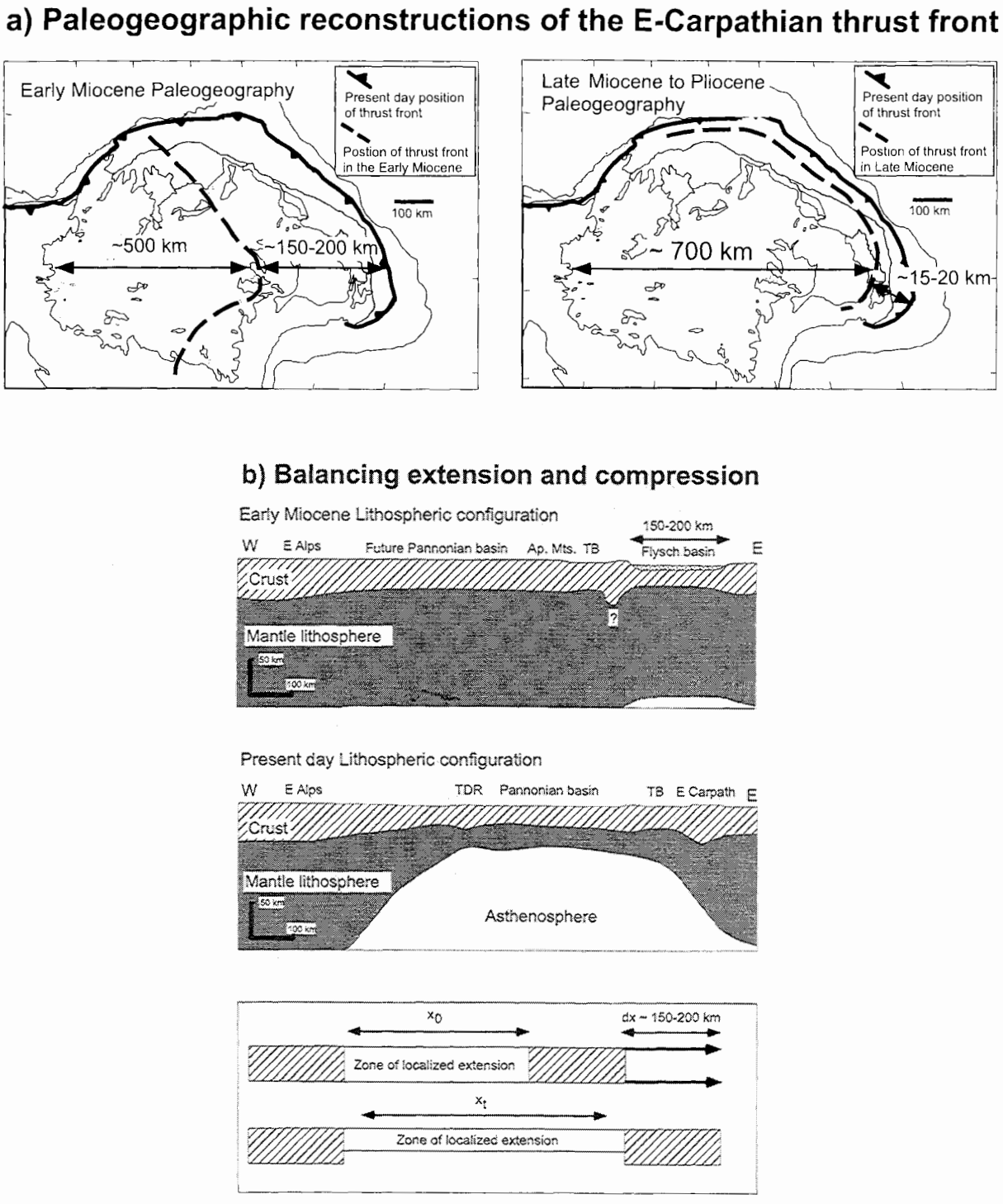

Figure 7. Estimates of Eastern Alps escape.(a) Paleogeographic reconstruction of the position of the east Carpathian thrust front in the Neogene [after *Ellouz et al.*, 1994]. (b) Balancing extension and compression in the Pannonian basin system. An estimate of the amount of Eastern Alps escape is obtained by balancing eastward translation of the east Carpathians with average extension in the Pannonian basin.

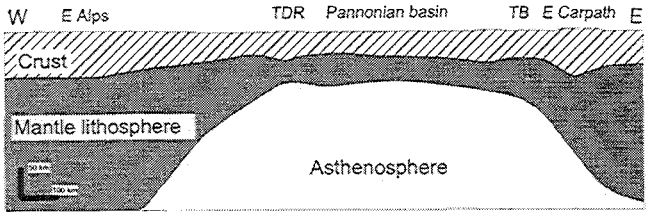

Figure 8. Present-day crust and lithosphere configuration along an E-W section through the Pannonian basin system [after *Horvath*, 1993].

escape is of minor importance for the Neogene extension history of the Pannonian basin system.

4. Finite Element Modeling of Small-Scale Convective Upwelling Following Passive Rifting

A two-dimensional (2-D) thermomechanical finite element model is applied to the Pannonian basin history to investigate the conditions of small-scale convective upwelling following the first passive rift phase. We consider an E-W section reaching from the Eastern Alps to the east Carpathians (Figure 8). Although the Pannonian basin exhibits notable 3-D features, overall extension and translation of the east Carpathians occurred in an E-W direction. It appears therefore, in a first approximation, justified to model the Pannonian basin history in a 2-D east-west section.

The equations of static equilibrium are solved in a 2-D plane strain thermomechanical model, with a pressure, temperature, and strain rate dependent visco-elasto-plastic rheology. Changes in the temperature field due to advection and conduction are calculated during run time. The temperature dependence of density is included.

Mechanical boundary conditions include horizontal velocities applied at the sides of the model with free slip in the vertical direction. The lower part of the model has been fixed in the vertical direction with free slip in the horizontal direction. The upper surface is free. Thermal boundary conditions include fixed temperatures at the surface and the lithosphere-asthenosphere boundary and zero lateral heat flux through the side boundaries. A more detailed description of the numerical model is given elsewhere [*Huismans*, 1999; *Huismans et al.*, 2001].

The model is composed of three layers which represent the upper crust, the lower crust, and the mantle. The nonlinear temperature-dependent viscous behavior of the model is determined by power law creep parameters of dry granite (upper crust), diabase rheology (lower crust), and dry olivine (mantle) [*Carter and Tsenn*, 1987]. Brittle behavior is modeled by a Mohr-Coulomb plastic flow criterion with parameters consistent with Byerlee's law Table 1). For the initial geometry and the mesh used, see Figure 9.

4.1. Boundary Conditions, Constraints, and Reference Model Description

The initial conditions for the modeling have been constrained by considering the prerift crust and lithosphere thickness and the initial width of the deforming zone. It is generally assumed that previous to the extensional history, the Pannonian crust and lithosphere had been moderately thickened [*Horvath*, 1993; *van Balen and Cloetingh*, 1995]. The prerift crustal thickness was of the order of 40-45 km [*Ratschbacher et al.*, 1991a; *van Balen and Cloetingh*, 1995], the prerift lithosphere thickness is less well constrained and may range from 120 to 200 km. The prerift width in E-W direction of the zone that experienced lithosphere thinning and basin formation, e.g., the zone between the Eastern Alps and the Apuseni Mountains, is of the order 200-350 km.

The first passive rift event is dated to have lasted from 17.5 to 14.0 Ma [*Horvath*, 1993]. Strong mantle lithosphere thinning and the second rift phase occurred

Table 1. Model Parameters

Symbol	Meaning	Value
E	Youngs modulus	10^{10} Pa
G	shear modulus	10^{10} Pa
ν	Poisson's ratio	0.25
ϕ	angle of friction	30°
ψ	angle of dilatation	0°
S_0	cohesion	2.10^7 Pa
ρ_{uc0}	density u-crust 0°C	2700 kg m^{-3}
ρ_{lc0}	density l-crust 0°C	2800 kg m^{-3}
ρ_{m0}	density mantle 0°C	3300 kg m^{-3}
α	thermal expansion	3.1 x 10^{-5} °C^{-1}
k	thermal conductivity	2.6 W m^{-1} C^{-1}
c_p	specific heat	1050 m^{-2} s^{-2} °C^{-1}
H	heat production	1 x 10^{-6} W m^{-2}
	Creep Parameters for Granite	
n_G	power law exponent	3.3
Q_G	activation energy	186.5 kJ mole^{-1}
A_G	initial constant	3.16 x 10^{-26}Pa^{-n} s^{-1}
	Creep Parameters for Diabase	
n_D	power law exponent	3.05
Q_D	activation energy	276 kJ mole^{-1}
A_D	initial constant	3.2 x 10^{-20} Pa^{-n} s^{-1}
	Creep Parameters for Dry Olivine	
n_O	power law exponent	3.0
Q_O	activation energy	510 kJ mole^{-1}
A_O	initial constant	7 x 10^{-14} Pa^{-n} s^{-1}

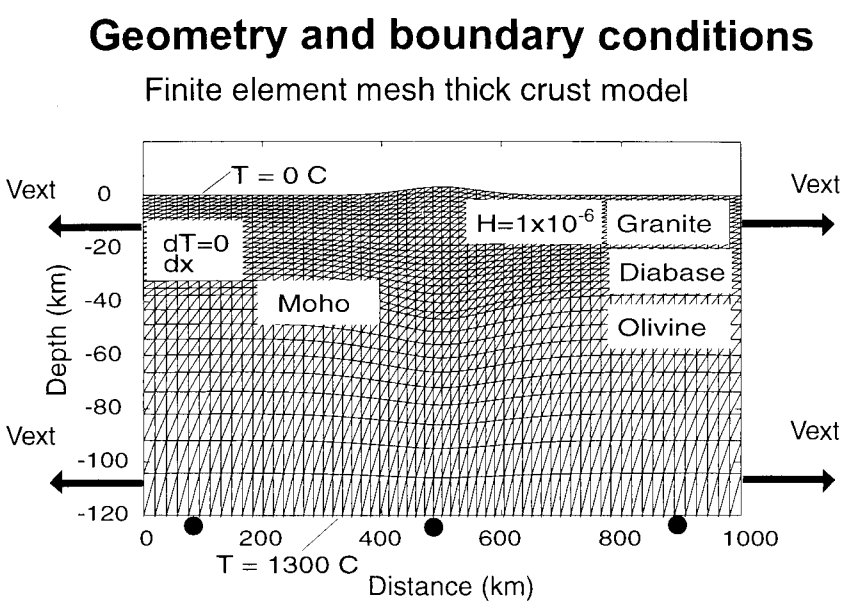

Figure 9. Finite element model setup, mesh and boundary conditions.

around 11.5-8(?) Myr B.P., 6-8 Myr following the start of the first rift phase. It has been demonstrated that 100-150 km of eastward movement of the east Carpathians occurred in the late early Miocene to late Miocene between 17.5 and 14-9.5 Myr B.P. [*Ellouz and Roca*, 1994]. We modeled three distinct scenarios based on these constraints in which the duration and amount of extension were varied (Table 2).

4.2. Description of the Reference Models

All of the models are characterized by a crustal thickness of 35 km, and in the absence of good constraints on the thickness of the lithosphere, each of the models has been run with a 120 km thick and with a 150 km thick lithosphere.

In the center of the models a 300 wide zone of the crust has been thickened to 45 km, representing the prerift thickened crust. A constant asthenosphere temperature of $T_a = 1300°C$ is applied at the bottom of the lithosphere. It is assumed that the prerift lithosphere was thermally equilibrated. After the relevant amount of extension has been reached, boundary velocities were lowered 1 order of magnitude, decreasing the amount of subsequent, far-field-related postrift extension to a minimum. Characteristics of the reference models are given in Table 3. To facilitate a comparison with the Pannonian basin history, the models start at 17.5 Ma and evolve until 0 Ma.

5. Modeling Results

5.1. Model 1a: 100 km Extension From 17.5 to 14 Ma, Normal 120 km Lithosphere

In Model 1 a total amount 100 km of extension takes place between 17.5 and 14 Ma. This results in a boundary velocities of 9.2×10^{-10}m s^{-1} during a period of 3.5 Myr. The model represents a situation in which most of the far-field-driven extension takes place during the first rift phase.

Plate 1 shows the situation at the end of the synrift, at 14 Ma, and at the end of the postrift, at 0 Ma. Stress

Table 2. Model Scenarios for Pannonian Basin

Model	Amount of Extension, km	Extension Duration, Ma	Velocity, m s^{-1}
1	100	3.5	9.2×10^{-10}
2	150	6.0	8.0×10^{-10}
3	100	8.0	4.0×10^{-10}

Table 3. Setup Reference Models

Parameter	value
Length of model x_L	1000 km
Depth base upper crust h_{uc}	15 km
Depth base upper crust h_{lc}	35 km
Depth base mantle lithosphere h_m	120 or 150 km
Thickened crust	45 km
Width of thickened zone	300 km
Temperature at the base T_{base}	1300 °C

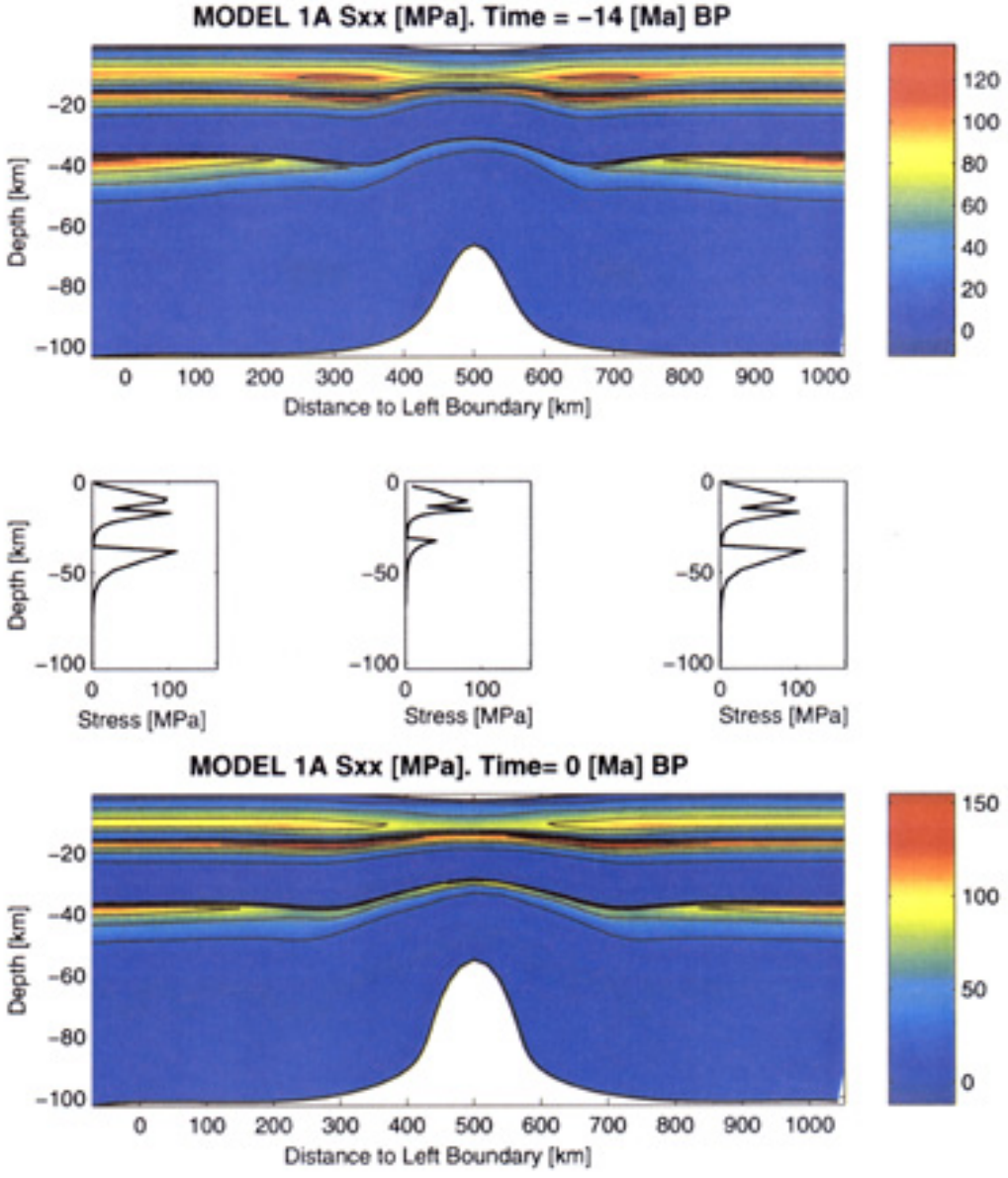

Plate 1. Model 1a: Horizontal deviatoric stress at 14 Ma (top panel) and at 0 Ma (bottom panel). At 14 Ma, far-field-velocity is reduced 1 order of magnitude, decreasing further far-field-related extension to a minimum.

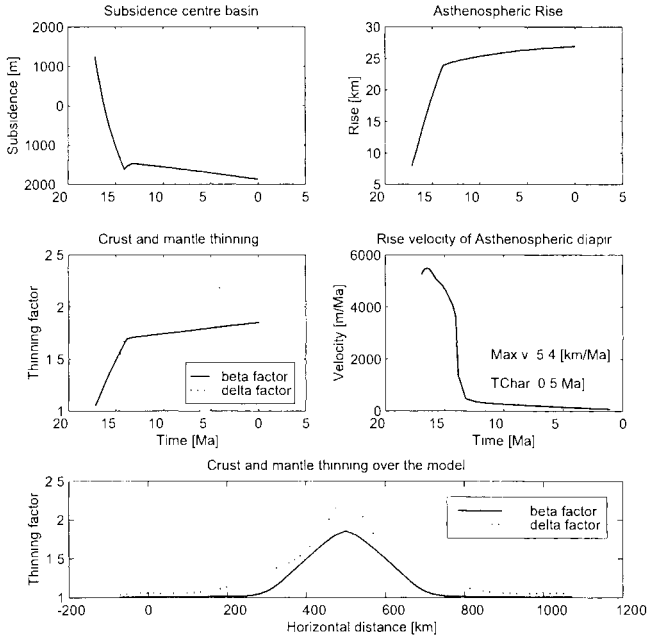

Figure 10. Model 1a: Predictions for vertical motions and thinning factors. Basin subsidence, asthenospheric rise, crust and mantle lithosphere thinning, and rise velocity of the asthenosphere diapir in the center of the model are given in the top and middle panels. The bottom panel gives crust and mantle lithosphere thinning β and δ over the model.

concentration has taken place in the upper crustal layers and in the upper part of the mantle lithosphere. A large reservoir of weak lower crust exists in the center of the model owing to the crustal thickening. It should be stressed that the thermal anomaly in the model is completely due to the increased heat production related to crustal thickening.

At 14 Ma a 150 km wide surface depression and 200 km wide broad upwelling of the asthenosphere have developed. Subsidence of the center of the basin area is of the order of 1700 m, whereas the asthenosphere diapir has risen 24 km. Significant thermal advection has taken place. Total extension amounts to 100 km. The crust has been thinned by a moderate thinning factor $\beta = 1.25$, whereas the mantle lithosphere has been thinned by a factor of $\delta = 2.0$.

Subsequently, boundary velocities are lowered 1 order of magnitude, limiting further far-field extension to a minimum. In the following interval the dome continues to rise an additional 3-4 km with much lower velocity. At 0 Ma, 17 Myr following the start of rifting (Plate 1 and Figure 10), total crustal thinning amounts to $\beta = 1.3$, whereas the mantle lithosphere has been thinned by a factor of $\delta = 2.5$. A peak rise velocity of the convective upwelling of 5.4 km Myr^{-1} is reached 1 Myr after the initiation of the rift. The crust and mantle thinning pattern (Figure 10) shows that during the synrift, crustal thinning is linearly increasing with time, whereas mantle lithosphere thinning shows a nonlinear increase of the thinning factor. This can be interpreted as the increasing importance of the convective upwelling with increasing perturbation due to the passive rift event.

5.2. Model 1b: 100 km Extension Between 17.5 and 14 Ma, Thick 150 km Lithosphere

In this model the thickness of the lithosphere has been increased to 150 km. Increasing the thickness of the mantle lithosphere has the effect of increasing the buoyancy forces and with this the potential small-scale convective instability of the system.

In Plate 2 the situations at 14 and at 3 Ma are shown. The total amount of crustal thinning is of the same order as in model 1a, whereas asthenospheric diapirism and the amount of additional postrift asthenospheric rise has increased. At the end of the synrift the crust has extended by a factor $\beta = 1.3$. The mantle lithosphere has been thinned by a factor of $\delta = 2.2$.

At 0 Ma, total subsidence in the center of the model is 1800 m, whereas the asthenosphere has risen 40 km. In the postrift the asthenosphere rises an additional 7-8 km, with a total mantle lithosphere thinning at 0 Ma of $\delta = 3.0$ compared with $\delta = 2.5$ in model 1a (Figure 11). The asthenospheric dome obtains its peak rise velocity 7.6 km Myr^{-1} at 2.3 Myr following the initiation of the rift. The peak rise velocity is higher but obtained later than in the previous model. This shows the effect of increased buoyancy forces, which increase the rise velocity, and the effect of the slightly colder thermal conditions due to thickening of the lithosphere, which slightly delays the acceleration of the diapir.

5.3. Model 2a: 150 km Extension Between 17.5 and 11.5 Ma, Normal 120 km Lithosphere

In Model 2 a total amount of 150 km of extension takes place during a period of 6.0 Myr. In comparison with the previous model this model is characterized by more extension taking place during a longer time interval at a similar velocity. The boundary velocities are 8.0 x 10^{-10}m s^{-1} during a period of 6.0 Myr. This model represents a situation in which most of the far-field-driven extension takes place between 17.5 and 11.5 Ma before present.

At 11.5 Ma, asthenospheric upwelling as well as crustal thinning are well developed (Figure 12). A relative narrow upwelling with a width of 200 km together with broad Moho updoming can be observed. Crustal thinning is of the order of $\beta = 1.6$, whereas the mantle lithosphere is thinned by a factor $\delta = 2.8$ (Figure 12). The center of the basin has subsided to a depth of 3000 m, whereas the asthenosphere has risen 30 km.

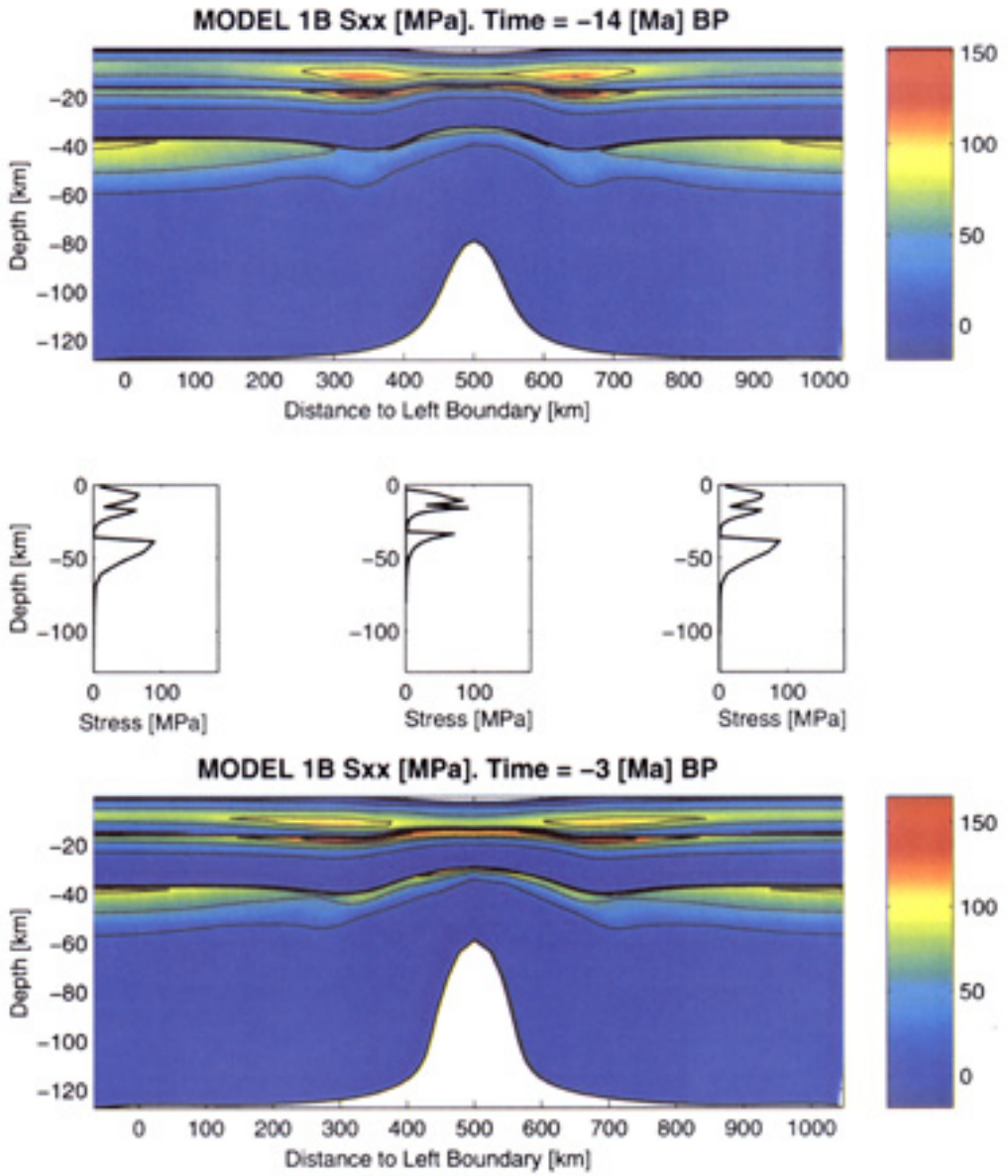

Plate 2. Model 1b: Horizontal deviatoric stress at 14 (top panel) and at 0 Ma (bottom panel). At 14 Ma, far-field-velocity is reduced 1 order of magnitude, decreasing further far-field-related extension to a minimum.

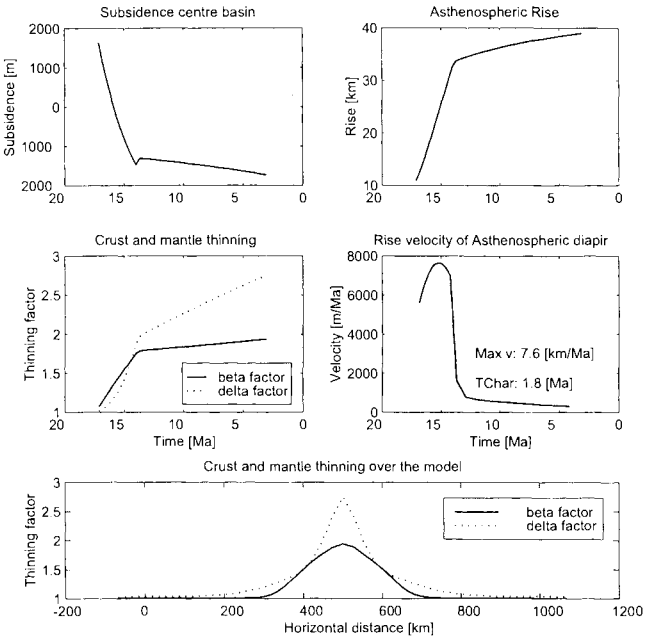

Figure 11. Model 1b: Predictions for vertical motions and thinning factors. Basin subsidence, asthenospheric rise, crust and mantle lithosphere thinning, and rise velocity of the asthenosphere diapir in the center of the model are given in the top and middle panels. The bottom panel gives crust and mantle lithosphere thinning β and δ over the model.

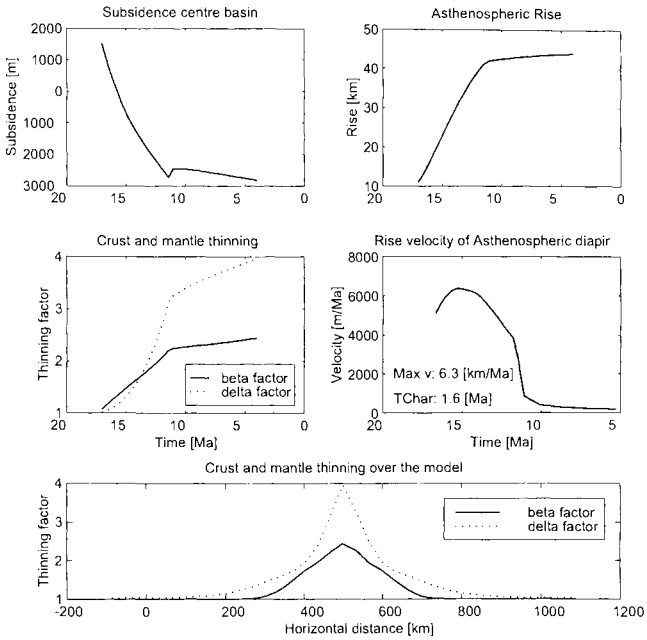

Figure 13. Model 2b: Predictions for vertical motions and thinning factors. Basin subsidence, asthenospheric rise, crust and mantle lithosphere thinning, and rise velocity of the asthenosphere diapir in the center of the model are given in the top and middle panels. The bottom panel gives crust and mantle lithosphere thinning over the model.

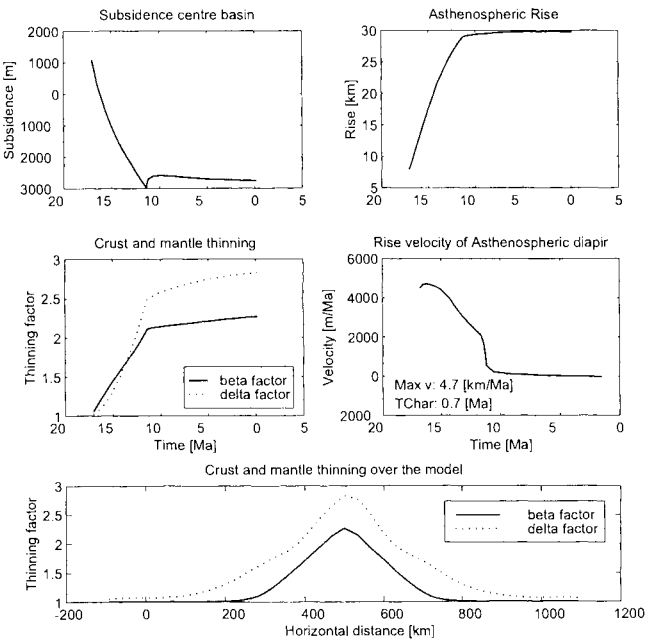

Figure 12. Model 2a: Predictions for vertical motions and thinning factors. Basin subsidence, asthenospheric rise, crust and mantle lithosphere thinning, and rise velocity of the asthenosphere diapir in the center of the model are given in the top and middle panels. The bottom panel gives crust and mantle lithosphere thinning over the model.

At 0 Ma, only moderate additional thinning has affected the mantle lithosphere and the crust. Since most of the possible small-scale convective asthenosphere upwelling occurred already during the synrift, only minor additional rise has taken place in the postrift evolution. The maximum asthenospheric rise velocity of 4.7 km Myr^{-1} is obtained 1.2 Myr after the initiation of the rift zone.

5.4. Model 2b: 150 km Extension Between 17.5 and 11.5 Ma, Thick 150 km Lithosphere

In model 2b the lithosphere thickness has been increased to 150 km. Again, the velocity and amount of asthenosphere upwelling are higher than in model 2a because of the larger buoyancy forces.

At 11.5 Ma, crust and mantle thinning factors are $\beta = 1.65$ and $\delta = 3.5$, respectively (Figure 13). The asthenosphere has risen 40 km and the basin has subsided to a depth of 2700 m. Mantle lithosphere thinning accelerates during the synrift and starts to deviate from the crustal thinning around 13.5 Ma (Figure 13). At 11.5 Ma, when the extensional boundary velocity is lowered 1 order of magnitude, rise velocity drops. However, since there is still accommodation space for the asthenospheric diapir in the upper part of the mantle lithosphere, upwelling continues. At 3.5 Ma, mantle

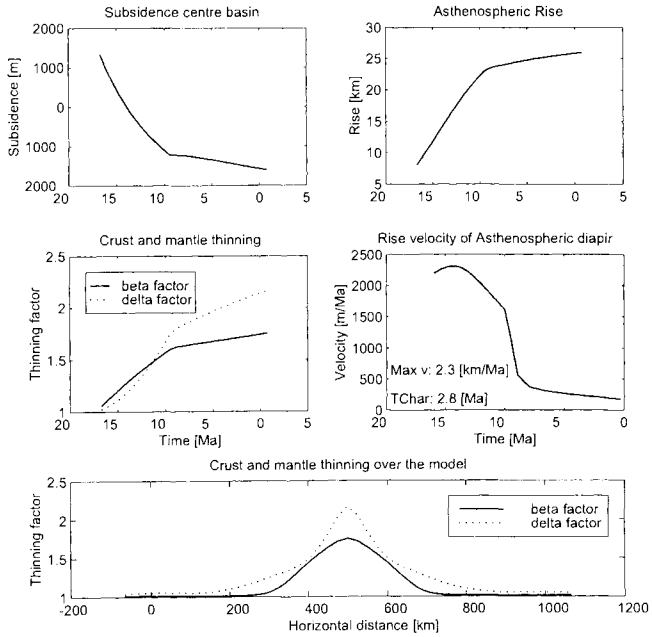

Figure 14. Model 3a: Predictions for vertical motions and thinning factors. Basin subsidence, asthenospheric rise, crust and mantle lithosphere thinning, and rise velocity of the asthenosphere diapir in the center of the model are given in the top and middle panels. The bottom panel gives crust and mantle lithosphere thinning over the model.

lithosphere thinning has increased to $\delta = 4.2$, whereas crustal thinning has only increased by a minor amount to $\beta = 1.7$ (Figure 13). The final morphology of the rift shows a relatively narrow focused asthenospheric upwelling with a wavelength of 150-200 km and 200 km wide surface depression.

5.5. Model 3a: 100 km Extension Between 17.5 and 9.5 Ma, Normal 120 km Lithosphere

In model 3a a total amount of 100 km of extension takes place during a period of 8 Myr. The only difference with model 1 is the lower velocity at which the extension takes place. The resulting boundary velocity is 4.0 x 10^{-10}m s^{-1} during a period of 8 Myr. This model represents a situation in which far-field-driven extension takes place during the first and second rift phases between 17.5 and 9.5 Ma.

At 9.5 Ma a wide, 1200 m deep surface depression and an asthenosphere upwelling with an amplitude of 23 km have developed (Figure 14). At this stage, crustal and mantle lithosphere thinning are of the order $\beta = 1.3$ and $\delta = 2.0$, respectively (Figure 14). During the subsequent rift history an additional 4-6 km of asthenosphere upwelling increases mantle lithosphere thinning to $\delta = 2.5$, whereas only minor additional thinning has affected the crustal layers. A maximum asthenosphere rise velocity of 2.3 km Myr^{-1} is reached at 3.3 Myr following the initiation of the rift zone. The crustal layers show minor thickening (i.e., $\beta < 1$) beneath the rift flanking regions.

5.6. Model 3b: 100 km Extension Between 17.5 and 9.5 Ma, Thick 150 km Lithosphere

Similarly, as in the results of Model 1b and 2b the amount and velocity of mantle lithosphere thinning increase with respect to the situation of a 120 km thick lithosphere (Figure 15). Here, at 9.5 Ma, the mantle lithosphere and the crust have been thinned by an amount of $\delta = 2.1$ and $\beta = 1.25$ (Figure 15). In the subsequent postrift evolution, additional thinning to $\delta = 3.0$ and $\beta = 1.3$ takes place. Post-rift additional rise of the asthenosphere in this model amounts to 6-8 km. The plot of the rise velocity shows that at 0 Ma the asthenospheric upwelling did not yet reach its limiting isotherm and will continue moving upward.

5.7. Model Inferences for Modes of Lithosphere Extension

Several conclusions may be drawn from the model results. The amount of crustal thinning is directly proportional to the amount of far-field extension with sim-

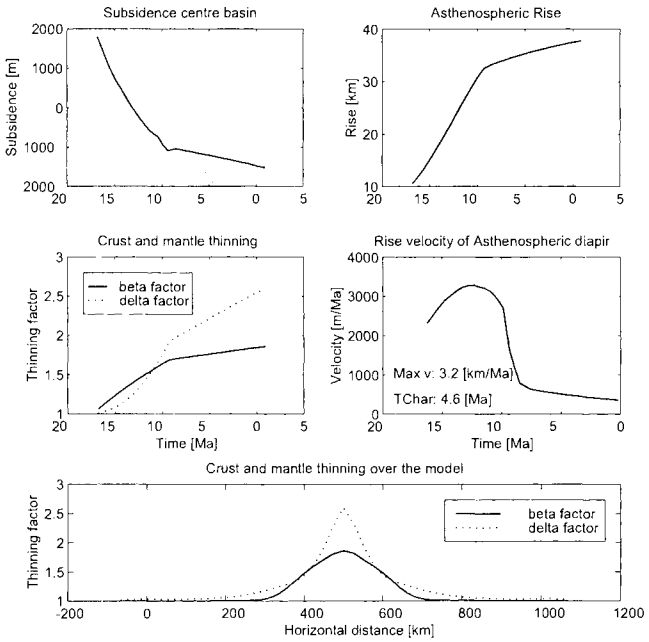

Figure 15. Model 3b: Predictions for vertical motions and thinning factors. Basin subsidence, asthenospheric rise, crust and mantle lithosphere thinning, and rise velocity of the asthenosphere diapir in the center of the model are given in the top and middle panels. The bottom panel gives crust and mantle lithosphere thinning over the model.

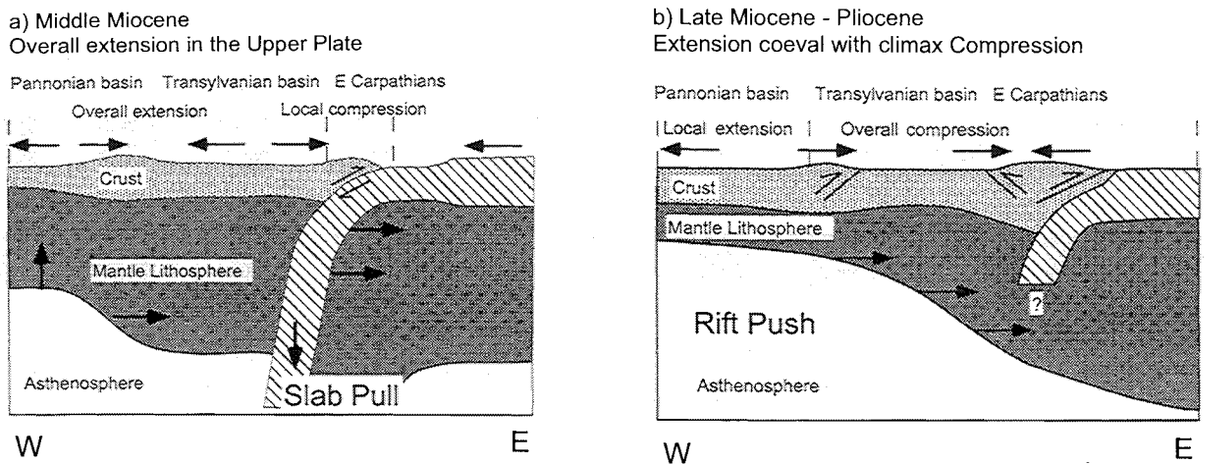

Figure 16. Observed stress patterns of the Pannonian basin and constraints given by the regional tectonic evolution of the Transylvanian basin. (a) First rift phase dominated by slab rollback and back arc extension (b) Second rift phase dominated by rift push due to asthenospheric upwelling.

ilar β values for models 1 and 3. Two factors determine the amount of mantle lithosphere thinning, i.e., a component of far-field extension related passive necking and a component of buoyancy-driven small-scale convective thinning. The relative contribution of these two components depends on the efficiency of the buoyancy-driven flow, which is, in turn, dependent on the temperature of the asthenosphere and the thickness of the lithosphere.

On the basis of the tectonic evolution, model 1b provides the most reasonable scenario. Here most of the far-field-driven extension takes place during the synrift phase, whereas substantial additional asthenospheric rise takes place in the postrift evolution. The constraints on the exact timing and amount of E-W directed extension do not justify a further fitting of the model to the Pannonian basin, which is also not realistic given the large uncertainties in the rheological parameters and the thermal conditions. The model results, however, show that using realistic rheological parameters and boundary conditions consistent with the tectonic evolution of the Pannonian basin, the two-stage extensional evolution of the Pannonian basin can be explained by a first passive rift phase followed by a phase of small-scale convective upwelling of the asthenosphere.

6. Discussion and Conclusions

6.1. First Rift Phase: Passive Rifting Owing to Back Arc Extension

Following the observations it is likely that the first phase of extensive strike slip and homogeneous extension is related to initiation of subduction and subsequent back arc extension, as proposed be many authors [*Stegena et al.*, 1975; *Royden et al.*, 1983b; *Horvath*, 1993].

The notion that the whole region toward the east Carpathian arc experienced overall E-W extension with only local contractional accretionary wedge tectonics in the east Carpathian arc suggests that subduction-related back arc extension is the dominant process during this time (Figure 16). As the prerift crust in the Pannonian region is thought to have had a moderately larger then normal thickness of around 40-45 km [*van Balen and Cloetingh*, 1995], gravitational collapse of the overthickened and thermally weakened crust in the Pannonian region may have assisted the overall east-west extension generated by the subduction system.

6.2. Second Rift Phase and Coeval Mountain Building in the East Carpathians: Small-Scale Convective Upwelling-Related Active Rifting

Several models have been invoked to explain the late mantle lithosphere thinning during the second rift phase and the coeval climax of compression. A mantle plume can be ruled out since in this case, alkaline volcanics and uplift are expected to precede the rift history, which is in contradiction with the observations. The observation that mantle lithosphere thinning occurred late in the rift history suggests a relation to the previous rift history. *Stegena et al.* [1975] suggested that thermal erosion of the mantle lithosphere was accomplished by asthenospheric melts triggered by the fluids expulsed from the surrounding subduction zones. The small amounts of alkaline melts [*Pecskay et al.*, 1995], however, contradict massive melting of the shallow asthenosphere and the lower lithosphere. Therefore the intrusion of melts can only account for a minor amount of thinning of the mantle lithosphere.

More recently, quantitative models of extensional basin formation have explored the possible role of lower crustal

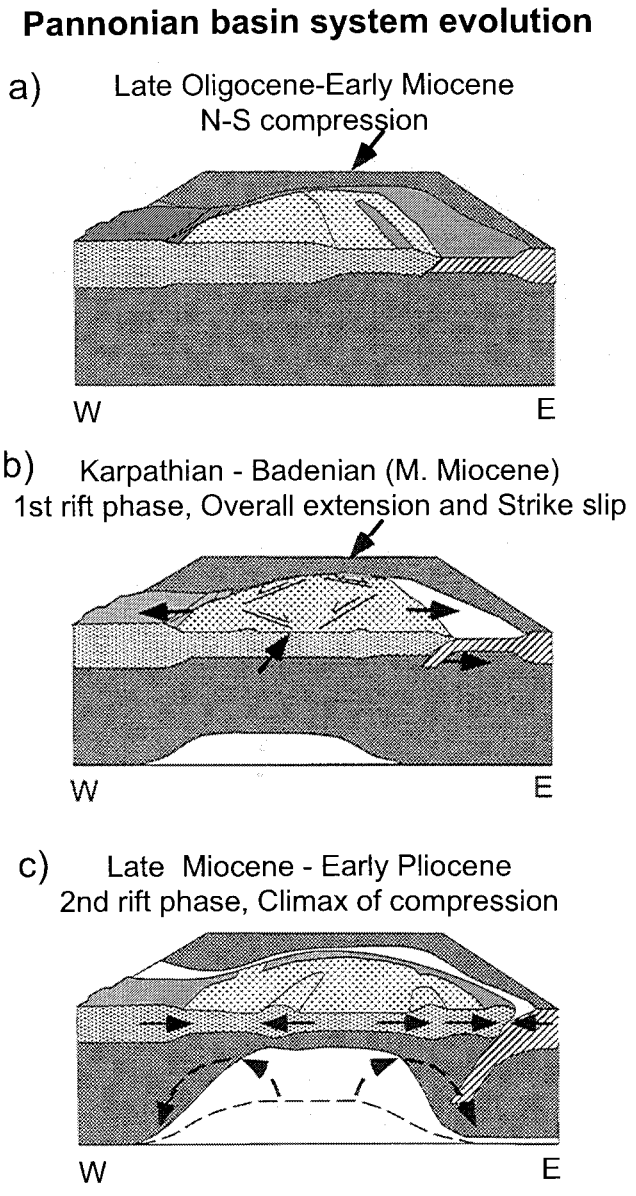

Figure 17. Three dimensional block diagrams summarizing the Pannonian basin evolution. (a) Late Oligocene-early Miocene prerift thickening. (b) First rift phase owing to passive rifting driven by slab rollback and associated back arc extension. (c) Second rift phase and coeval compression owing to asthenosphere doming and associated increase of the rift push forces.

flow toward the rift flanks in response to Moho uplift [*Moretti and Pinet,* 1987] or in response to surface processes, where erosion of the rift flanks may enhance lower crustal thinning in the basin area [*Burov and Cloetingh,* 1997]. Such processes potentially explain the observed differential thinning of the lower crust with respect to the upper crust [*Stegena et al.,* 1975]. The amount of syntectonic erosion of the rift flanks in the Pannonian basin appears to be low but is not very well constrained. It is therefore at present difficult to asses the potential role of surface process on the rift basin evolution. It appears, however, difficult to explain the high differential thinning of the mantle lithosphere in the area with these kind of processes alone.

The finite element modeling shows that small-scale convective upwelling following a first phase of passive rifting may explain the late synrift to postrift mantle lithosphere thinning in the Pannonian basin area. The model results show that the timescale and amount of asthenosphere upwelling in the Pannonian basin are consistent with a normal mantle temperature of T_a = 1300°C. The thermal anomaly in the model provided by thick crust and by the thermal advection given by the first passive rift phase drives the small-scale convective upwelling. It should be emphasized that no external heat source (e.g., mantle plume) is needed to drive the convective flow.

6.3. Rift Push Forces Driving Second Phase of Extension and Coeval Climax of Contraction

The coeval occurrence of the second rift phase with the strong mantle lithosphere upwelling suggests a causal relation between these two processes. If peak mantle lithosphere thinning in the time interval of the inversion phase and the second rift phase, i.e., in the late Miocene around 13-10 Ma, is indeed related to active asthenosphere upwelling, it appears straightforward to connect the second rift phase to the dynamics of doming. This is not an unexpected relationship since the buoyancy forces related to rifting generate a net extensional rift push force [*Turcotte,* 1983; *Turcotte and Emerman,* 1983; *Le Pichon and Alvarez,* 1984; *Huismans,* 1999]. Additionally, differential thinning of the lithosphere implies a drastic increase of the rift push forces to the order of magnitude of plate driving forces.

A second reason to interpret rift push as the dominant force during this time interval is given by the stress and strain distribution for the late Miocene-early Pliocene. Most previous models suggested that the compressional and extensional forces in the Pannonian basin system are only related to subduction in the east Carpathian arc and to the northward push of the Adriatic plate. These models, however, have difficulty to explain compressional stresses far in the overlying plate coeval with the second phase of extension. That is, the Transylvanian basin, which forms the 200 km wide transition zone between the Pannonian basin and the east Carpathian arc, is affected by strong contractional deformation during this time (Figure 16b).

This suggests that the main driving force for the compression is located in the central Pannonian basin, e.g., in the area affected by strong mantle lithosphere upwelling at this time. This matches the expected stress and strain pattern for a situation dominated by rift push, which is given by local extension affecting the

rifting area and overall compression affecting the region around it (Figure 16b). Thus the regional stress and strain pattern for the late Miocene-early Pliocene is consistent with the rift push forces being dominant over the forces related to the subduction in the east Carpathian arc.

The available driving forces for extensional and contractional deformation play a key role in the sequence of events which delineate the Neogene evolution of the Pannonian basin system. The first phase of extension is compatible with the combined effects of initiation of subduction beneath the east Carpathian arc and extensional collapse of the overthickened crust of the Pannonian prerift lithosphere (Figures 17a and 17b). The second phase of extension in the Pannonian basin associated with strong asthenosphere upwelling has been explained here in terms of small-scale convective upwelling of the mantle lithosphere triggered by the first rift event (Figure 17c).

Acknowledgments. Frank Horvath and Laszlo Csontos are thanked for constructive discussions. Anco Lankreijer is thanked for permission to show subsidence analysis results for the Pannonian basin. Giorgio Ranalli and Evgene Burov are thanked for their constructive comments on the manuscript. R. S. Huismans was supported by the Netherlands Organisation of Scientific Research (NWO), project 751.360.003. Netherlands Research School of Sedimentary Geology publication 20010306.

References

Balogh, K., F. Ebner, and C. Ravasz, K/Ar Alter tertiarer Vulkanite der sudostlichen Steiermark und des sudlichen Burgenlandes, in *Jubilaumschrift 20 Jahre Geologische Zusammenarbeit Österreich-Ungarn,* vol. 2, pp. 55-72, Österreichische Mineralogische Gesellschaft, Wien, 1994.

Beaumont, C., C.E. Keen, and R. Boutilier, On the evolution of rifted continental margins: Comparison of models and observations for the Nova Scotian margin, *Geophys. J. R. Astron. Soc., 70,* 667-715, 1982.

Bergerat, F., From pull-apart to the rifting process: The formation of the Pannonian basin, *Tectonophysics, 157,* 271-280, 1989.

Buck, W. R., When does small-scale convection begin beneath oceanic lithospere?, *Nature, 313,* 775-777, 1985.

Buck, W.R., Small-scale convection induced by passive rifting: The cause for uplift of rift shoulders, *Earth Planet. Sci. Lett., 77,* 3-4, 1986.

Burov, E., and S. Cloetingh, Erosion and rift dynamics: New thermomechanical aspects of postrift evolution of extensional basins, *Earth Planet. Sci. Lett., 150,* 7-26, 1997.

Carter, N. L., and M. C. Tsenn, Flow properties of continental lithosphere, *Tectonophysics, 136,* 27-63, 1987.

Cloetingh, S., and R. Wortel, Stress in the Indo-Australian plate, *Tectonophysics, 132,* 49-67, 1986.

Csontos, L., Tertiary tectonic evolution of the Intra-Carpathian area: A review, *Acta Vulcanol., 7,* 1-15, 1995.

Csontos, L., G. Tari, F. Bergerat, and L. Fodor, Evolution of the stress fields in the Carpatho-Pannonian area during the Neogene, *Tectonophysics, 199,* 73-91, 1991.

Dobosi, G., R.V. Fodor, and S.A. Goldberg, Late Cenozoic alkalic basalt magmatism in northern Hungary and Slovakia: Petrology, source compositions and relationships to tectonics, *Acta Vulcanol., 7,* 199-208, 1995.

Downes, H., and O. Vaselli, The lithospheric mantle beneath the Carpathian-Pannonian Region: A review of trace element and isotopic evidence from ultramafic xenoliths, *Acta Vulcanol., 7,* 219-229, 1995.

Ellouz, N., and E. Roca, Palinspastic reconstructions of the Carpathians and adjacent areas since the Cretaceous: A quantitative approach, in *Peri-Tethyan Platforms,* edited by F. Roure, pp. 51-78, Editions Technip, Paris, 1994.

Embey-Isztin, A., and G. Dobosi, Mantle source characteristics for Miocene-Pliocene alkali basalts, Carpathian-Pannonian region: A review of trace elements and isotopic compositions, *Acta Vulcanol., 7,* 155-166, 1995.

Fodor, L., From transpression to transtension; Oligocene-Miocene structural evolution of the Vienna basin and the east Alpine-west Carpathian junction, *Tectonophysics, 242,* 151-182, 1995.

Fodor, L., L. Csontos, G. Bada, I. Gyorfi, and L. Benkovics, Tertiary tectonic evolution of the Pannonian basin and neighbouring orogens: A new synthesis of paleostress data, *Geol. Soc. Spec. Publ., 134,* 295-334, 2000.

Hippolyte, J.-C., and M. Sandulescu, Paleostress characterisation of the Wallachian phase in its type area (south eastern Carpathians, Romania), *Tectonophysics, 263,* 235-248, 1996.

Horvath, F., Towards a mechanical model for the formation of the Pannonian Basin, *Tectonophysics, 226,* 333-357, 1993.

Horvath, F., Phases of compression during the evolution of the Pannonian Basin and its bearing on hydrocarbon exploration, *Mar. Petrol. Geol., 12,* 837-844, 1995.

Houseman, G., and P. England, A dynamical model of lithosphere extension and sedimentary basin formation, *J. Geophys. Res., 91,* 719-729, 1986.

Huismans, R.S., Dynamic modeling of the transition from passive to active rifting, application to the Pannonian basin, Ph.D. thesis, 196 pp., Vrije Univ., Amsterdam, 1999.

Huismans, R.S., G. Bertotti, D. Ciulavu, C.A.E. Sanders, S.A.P.L. Cloetingh, and C. Dinu, Structural evolution of the Transylvanian Basin (Romania): A sedimentary basin in the bend zone of the Carpathians, *Tectonophysics, 272,* 249-268, 1996.

Huismans, R.S., Y.Y. Podladchikov, and S.A.P.L. Cloetingh, Pannonian Basin syn- and post-rift evolution: Dynamic modeling of the transition from passive to active rifting, *Przegl. Geol., 45,* 1078, 1997.

Huismans, R.S., Y.Y. Podladchikov and S. Cloetingh, Transition from passive to active rifting: Relative importance of asthenospheric doming and passive extension of the lithosphere, *J. Geophys. Res., 106,* 11,271-11,292, 2001.

Keen, C.E., The dynamics of rifting: Deformation of the lithosphere by active and passive driving forces, *Geophys. J. R. Astron. Soc., 80,* 95-120, 1985.

Keen, C.E., and R.R. Boutilier, Lithosphere-asthenosphere interactions below rifts, in *Rifted Ocean-Continent Boundaries,* edited by E. Banda, pp. 17-30, Kluwer Acad., Norwell, Mass., 1995.

Kooi, H., Tectonic modeling of extensional basins: the role of lithospheric flexure, intraplate stress and relative sealevel change, Ph.D. thesis, 183 pp., Vrije Univ., Amsterdam, 1991.

Lankreijer, A., M. Kovac, S. Cloetingh, P. Pitonak, M. Hloska, and C. Biermann, Quantitative subsidence analysis and forward modeling of the Vienna and Danube basins: Thin-skinned versus thick-skinned extension, *Tectonophysics, 252,* 433-451, 1995.

Le Pichon, X., and F. Alvarez, From stretching to subduction in back arc regions: Dynamic considerations, *Tectonophysics, 102,* 343-357, 1984.

Lenkey, L., Geothermics of the Pannonian Basin and its bearing on the tectonics of basin evolution, Ph.D. thesis, 214 pp., Vrije Univ., Amsterdam, 1999.

Matenco, L., Tectonic evolution of the Outer Romanian Carpathians; constraints from kinematic analyses and flexural modeling, Ph.D. thesis, 160 pp., Vrije Univ., Amsterdam, 1997.

McKenzie, D., Some remarks on the development of sedimentary basins, *Earth Planet. Sci. Lett., 40,* 25-32, 1978.

Moretti, I., and B. Pinet, Discrepancy between lower and upper crustal thinning, in *Sedimentary Basins and Basin-forming Mechanisms,* edited by C. Beaumont and A.J. Tankard, *Can. Soc. Pet. Geol. Mem., 12,* 233-239, 1987.

Muller, B., M.L. Zoback, K. Fuchs, L. Mastin, S. Gregersen, N. Pavoni, O. Stephannson, and C. Ljunggren, Regional pattern of tectonic stress in Europe, *J. Geophys. Res., 97,* 11,783-11,803, 1992.

Pecskay, Z., et al., Space and time distribution of Neogene-Quaternary volcanism in the Carpatho-Pannonian region, *Acta Vulcanol., 7,* 15-28, 1995.

Peresson, H., and K. Decker, Far field effects of late Miocene subduction in the eastern Carpathians: E-W compression and inversion of structures in the Alpine Carpathian Pannonian region, *Tectonics, 16,* 38-56, 1997a.

Peresson, H., and K. Decker, The Tertiary dynamics of the northern Eastern Alps (Austria): Changing paleostress in a collisional plate boundary, *Tectonophysics, 272,* 125-157, 1997b.

Ratschbacher, L., O. Merle, P. Davy, and P. Cobbold, Lateral extrusion in the Eastern Alps, part 1, Boundary conditions and experiments scaled for gravity, *Tectonics, 10,* 245-256, 1991a.

Ratschbacher, L., W. Frisch, H.G. Linzer, and O. Merle, Lateral extrusion in the Eastern Alps, part 2, Structural analysis, *Tectonics, 10,* 257-271, 1991b.

Ratschbacher, L., H.G. Linzer, F. Moser, R.O. Strusievicz, H. Bedelean, N. Har, and P.A. Mogos, Cretaceous to Miocene thrusting and wrenching along the central south Carpathians due to a corner effect during collision and orocline formation, *Tectonics, 12,* 855-873, 1993.

Rögl, F., Stratigraphic correlation of the Parathetys Oligocene and Miocene, *Mitt. Ges. Geol. Bergbaustud. Österr., 41,* 65-73, 1996.

Royden, L., and C.E. Keen, Rifting process and thermal evolution of the continental margin of eastern Canada determined from subsidence curves, *Earth Planet. Sci. Lett., 51,* 343-361, 1980.

Royden, L.H., F. Horvath, and B.C. Burchfiel, Transform faulting, extension, and subduction in the Carpathian Pannonian region, *Geol. Soc. Am. Bull., 93,* 717-725, 1982.

Royden, L., F. Horvath, A. Nagymarosy, and L. Stegena, Evolution of the Pannonian Basin system, 1, Tectonics, *Tectonics, 2,* 63-90, 1983a.

Royden, L., F. Horvath, A. Nagymarosy, and L. Stegena, Evolution of the Pannonian Basin system, 2, Subsidence and thermal history, *Tectonics, 2,* 91-137, 1983b.

Sachsenhofer, R.F., A. Lankreijer, S. Cloetingh, and F. Ebner, Subsidence analysis and quantitative basin modeling in the Styrian basin (Pannonnian Basin system, Austria), *Tectonophysics, 272,* 175-196, 1997.

Sanders, C., P. Andriessen, and S. Cloetingh, Life cycle of the east Carpathian orogen, erosion of a doubly vergent critical wedge assessed by fission track thermochronology, *J. Geophys. Res., 104,* 29,095-29,112, 1999.

Sclater, J.G., L. Royden, F. Horvath, B.C. Burchfiel, S. Semken, and L. Stegena, The formation of the intra-Carpathian basins as determined from subsidence data, *Earth Planet. Sci. Lett., 51,* 139-162, 1980.

Sengor, A.M.C., and K. Burke, Relative timing of rifting and volcanism on Earth and its tectonic applications, *Geophys. Res. Lett., 5,* 419-421, 1978.

Stegena, L., B. Geczy, and F. Horvath, Late Cenozoic evolution of the Pannonian Basin, *Tectonophysics, 26,* 71-90, 1975.

Szabo, C., S. Harangi, and L. Csontos, Review of Neogene and Quaternary volcanism of the Carpathian-Pannonian region, *Tectonophysics, 208,* 1-3, 1992.

Turcotte, D.L., Driving mechanisms of Mountain building, in *Controversy in Geology,* edited by K. Hsu, pp. 141-146, Academic Press, San Diego, Calif., 1983.

Turcotte, D.L., and S.H. Emerman, Mechanisms of active and passive rifting, *Tectonophysics, 94,* 39-50, 1983.

van Balen, R.T., and S. Cloetingh, Neural network analyses of stress-induced overpressures in the Pannonian Basin, *Geophys. J. Int., 121,* 532-544, 1995.

van Bemmelen, R.W., Geodynamic models for the Alpine type of orogeny (Test case II: The Alps in central Europe), *Tectonophysics, 18,* 33-79, 1973.

Vaselli, O., H. Downes, M. Thirlwall, G. Dobosi, N. Coradossi, I. Seghedi, A. Szakacs, and R. Vannucci, Ultramafic xenoliths in Plio-Pleistocene alkali basalts from the eastern Transylvanian Basin: Depleted mantle enriched by vein metasomatism, *J. Petrol., 1,* 23-53, 1995.

S. A. P. L. Cloetingh, Institute of Earth Sciences, Vrije Universiteit, de Boelelaan 1085, 1081 HV Amsterdam, Netherlands. (cloeting@geo.vu.nl)

R. S. Huismans, Department of Oceanography, Dalhousie University, Halifax, Nova Scotia, Canada, B3H 4J1. (ritske.huismans@dal.ca)

Y. Podladchikov, Geologisches Institut, ETH-Zentrum, Sonnegstrasse 5, CH 8092 Zurich, Switzerland. (yura@erdw.ethz.ch)

(Received November 28, 2000;
revised April 4, 2001;
accepted April 11, 2001.)